



APPLICABILITY OF DYNAMICAL STATISTICAL DOWNSCALING TO WIND PREDICTION ALONG RAILWAY

Yayoi Misu^{1,2}, Atsushi Yamaguchi³, and Takeshi Ishihara⁴

¹ Assistant Manager, Disaster Prevention Research Laboratory,
East Japan Railway Company

² Doctoral Student, Department of Civil Engineering, The University of Tokyo
7-3-1 Hongo, Bunkyo, Tokyo, 113-8656 JAPAN, misu@bridge.t.u-tokyo.ac.jp

³ Research Associate, Department of Civil Engineering, The University of Tokyo
7-3-1 Hongo, Bunkyo, Tokyo, 113-8656 JAPAN, atsushi@bridge.t.u-tokyo.ac.jp

⁴ Professor, Department of Civil Engineering, The University of Tokyo
7-3-1 Hongo, Bunkyo, Tokyo, 113-8656 JAPAN, ishihara@bridge.t.u-tokyo.ac.jp

ABSTRACT

The applicability of Dynamical Statistical Downscaling Procedure to wind prediction along railway tracks was examined. By combining a mesoscale wind climate database with a non-linear flow simulation model, MASCOT, the prediction of the wind climate at any sites along the railway track in Japan was made possible. The predicted results showed better agreements with the measurement than the results by simply using the mesoscale wind climate database and an empirical formula. Considering the effects of the surrounding structures by the wind tunnel test improved the prediction accuracy.

KEYWORDS: *DISASTER PREVENTION FOR RAILWAY, WIND CLIMATE ASSESSMENT,
DYNAMICAL STATISTICAL DOWNSCALING PROCEDURE, WIND TUNNEL TEST*

Introduction

In order to improve the safety level of train for cross wind that might cause derailment or turnover of the train with maintaining the punctuality of train schedules, the train operation should be regulated appropriately and countermeasures such as the installation of wind fences at strong wind prone sites should be conducted reasonably. It is important to specify the location and frequency of the strong wind along the railway tracks. The onsite measurement at certain places has been widely used for this purpose. However, it has limitation that it cannot measure the wind where an anemometer is not installed. Methods are, therefore, required to assess the spatial distribution of the strong wind events along the railway tracks.

A non-linear flow simulation model, MASCOT (Microclimate Analysis System for COmplex Terrain) was developed by Ishihara *et al.* (2003) to predict micro-scale wind climates on complex and steep terrain. In order to assess local wind climate without using onsite measurement, Yamaguchi *et al.* (2003) proposed Dynamical Statistical Downscaling Procedure based on the Idealizing and Realizing Approach with MASCOT. This procedure was developed for wind energy applications in which the main interest is wind speed at the hub-height such as 70m above ground. For railway applications, however, wind speed at lower height such as 5m is required, where the wind would be more strongly affected by surrounding obstacles.

In this study, the applicability of Dynamical Statistical Downscaling to wind assessment along railway for the height of 5m above ground was verified using the measured

wind speed. In addition, the effects of the surrounding structures such as embankments and wind fences that cannot be considered by the resolution of MASCOT was examined by the wind tunnel test to improve the prediction accuracy.

Measurement sites

In order to verify the accuracy of the proposed climate assessment method, the prediction results were compared with the measured wind speed and direction at three sites, near Kurihashi station on the JR Tohoku line. The map of the measurement sites are shown in Figure 1, and summarized in Table 1.

Empirical model for wind prediction

In this section, the applicability of the mesoscale wind climate database to assess the wind climate near the ground surface by using the empirical model is investigated. The outline of the mesoscale wind climate database is described in Table 2. It provides the frequency distribution of wind speed for each 12 wind speed bins and 16 wind direction sectors at 30m, 50m and 70m above ground with the horizontal resolution of 500m. Since wind climate at the height of 5m is needed for the railway applications, the wind speed profile was assumed to follow the power law and the power exponent was assumed to be a function of surrounding surface roughness. In addition to the height correction, the correction factors for embankment, cut or wind prevention forest were also considered. The wind prediction model can be written as

$$U = U_0 E F_e F_c F_f \quad (1)$$

where U_0 is the wind speed in the mesoscale wind climate database at 30m above ground, E is the height correction factor based on the power law. F_e , F_c and F_f are the correction factor of embankment, cut or vegetation as shown in Table 3.

The correction factor for the embankment F_e , was calculated by empirical formula for small terrain [Architectural Institute of Japan 2004] as.

$$F_e = (C_1 - 1) \left\{ C_2 \left(\frac{5}{H} - C_3 \right) + 1 \right\} \exp \left\{ -C_2 \left(\frac{5}{H} - C_3 \right) \right\} + 1 \quad (2)$$

where C_1 , C_2 and C_3 are the model parameters as functions of height, scale and slope of the terrain, the detail of which is described in [Architectural Institute of Japan 2004]. The

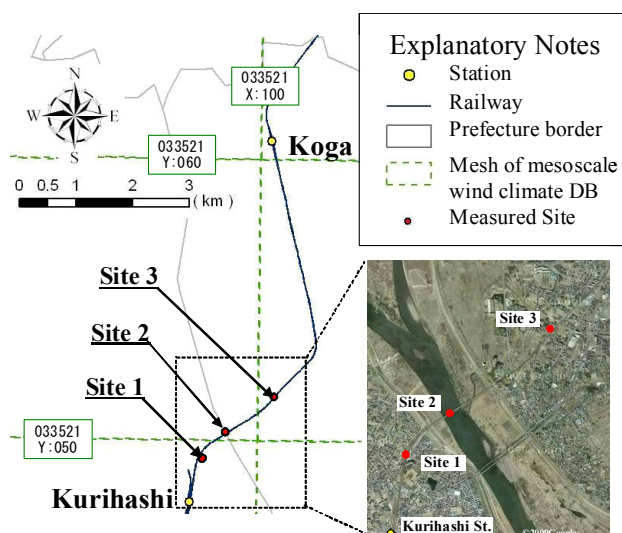


Figure 1. Schematic map of measured points

Table 1. Summary of the examined points

Site	Structure	Height[m]	Fences	Height of Fence [m]
1	Embankment	7.83	Exist	3
2	Bridge	9.77	Exist	3
3	Embankment	2.34	No	-

Table 2. The mesoscale wind climate database

Number and interval of the bins	12 bins with 1m/s interval
Number of wind direction sectors	16
Horizontal resolution	500m
Available height	30m, 50m, 70m

Table 3. Correction factors for empirical model

Structure	If it exist
Embankment (F_e)	$F_e = f(C_1, C_2, C_3, H)$
Cut (F_c)	0.9
Wind Prevention Forest (F_f)	0.9

correction factor for the cut F_c and the wind prevention forest F_f are based on [ECCS 1978] and [Tani 1974].

Wind prediction model based on Dynamical Statistical Downscaling

One of the limitations of the use of the mesoscale wind climate database is that it is based on the mesoscale meteorological simulation with the horizontal resolution of 500m, which means that it cannot take the effect of microscale terrains into account. In order to include this effect, Dynamical Statistical Downscaling Procedure (DSDP) based on Idealizing and Realizing Approach (IRA) [Yamaguchi *et al.* 2003] with a non-linear flow simulation model, MASCOT was carried out. It assumes a wind speed profile at the inflow boundary condition, where the terrain is assumed to be flat and have constant roughness length, and calculate the relative wind speed and change of the wind direction over the terrain. This calculation is iterated for all the wind direction sectors.

Wind speed near the ground surface is affected by microscale terrain, surrounding surface roughness, surrounding buildings, structures along railway, and wind break facilities. The affected wind speed can be written as

$$U = U_0 C_t C_s C_b \quad (3)$$

where U_0 is the wind speed in the mesoscale wind climate database at 30m above ground, C_t is a correction factor related to the effect of microscale terrain, surrounding surface roughness, and surrounding buildings. C_s is a correction factor related to the effect of a structure along the railway, and C_b is that of wind break facilities as shown in Table 4. C_t can be derived by the Dynamical Statistical Downscaling Procedure with MASCOT, and C_s and C_b can be derived by wind tunnel test.

Table 4. Correction factors for proposed model

Factor	Effect
C_t	microscale terrain, surrounding surface roughness, and surrounding buildings
C_s	structure along the railway
C_b	wind break facilities

A non-linear flow simulation model, MASCOT

In order to predict microscale wind climates on complex and steep terrain, a non-linear flow simulation model, MASCOT (Microclimate Analysis System for COMplex Terrain) was developed by Ishihara *et al.* (2003) MASCOT is based on Computational Fluid Dynamics (CFD) and solves Navier-Stokes equations numerically by assuming k - ϵ turbulence model. The governing equations of this model are as follows:

$$\frac{\partial \rho}{\partial t} + \frac{\partial \rho \bar{u}_j}{\partial x_j} = 0 \quad (4)$$

$$\frac{\partial \rho \bar{u}_i}{\partial t} + \frac{\partial \rho \bar{u}_j \bar{u}_i}{\partial x_j} = -\frac{\partial \bar{p}}{\partial x_i} + \frac{\partial}{\partial x_j} \left(\mu \frac{\partial \bar{u}_i}{\partial x_j} - \overline{\rho u'_i u'_j} \right) \quad (5)$$

where \bar{u}_i and u'_i are the average wind speed and fluctuating wind speed in the x_i direction. \bar{p} is the pressure, ρ is the density, and μ is the viscosity coefficient

Reynolds stress $-\overline{\rho u'_i u'_j}$ can be approximated by the linear eddy viscosity model.

$$\overline{\rho u'_i u'_j} = \frac{2}{3} \rho k \delta_{ij} - \mu_t \left(\frac{\partial u_i}{\partial x_j} + \frac{\partial u_j}{\partial x_i} \right) \quad (6)$$

Turbulent viscosity coefficient μ_t can be expressed using turbulent energy k and the rate of turbulent energy dissipation ϵ , which can be obtained by following equations.

$$\mu_t = C_\mu \rho \frac{k^2}{\varepsilon} \tag{7}$$

$$\frac{\partial \rho k}{\partial t} + \frac{\partial \rho \bar{u}_j k}{\partial x_j} = \frac{\partial}{\partial x_j} \left[\left(\mu + \frac{\mu_t}{\sigma_k} \right) \frac{\partial k}{\partial x_j} \right] - \rho \overline{u'_i u'_j} \frac{\partial \bar{u}_i}{\partial x_j} - \rho \varepsilon \tag{8}$$

$$\frac{\partial \rho \varepsilon}{\partial t} + \frac{\partial \rho \bar{u}_j \varepsilon}{\partial x_j} = \frac{\partial}{\partial x_j} \left[\left(\mu + \frac{\mu_t}{\sigma_\varepsilon} \right) \frac{\partial \varepsilon}{\partial x_j} \right] - C_{\varepsilon 1} \frac{\varepsilon}{k} \rho \overline{u'_i u'_j} \frac{\partial \bar{u}_i}{\partial x_j} - C_{\varepsilon 2} \frac{\rho \varepsilon^2}{k} \tag{9}$$

The constants C_μ , $C_{\varepsilon 1}$, $C_{\varepsilon 2}$, σ_k , and σ_ε are assigned to standard values 0.09, 1.44, 1.92, 1.0, and 1.3 respectively. The outline of MASCOT that used in this study is shown in Table 5.

Figure 2 shows the computational domain used in MASCOT. An analytical domain is set including a target domain which is a square with a side 10km. An additional domain is also set at upwind of the analytical domain and buffer zones are laid all around these domains. Table 6 shows calculation conditions of MASCOT. In order to improve the accuracy of the calculation at a target site, finer meshes are used in the target domain.

Table 5. The outline of MASCOT

Coordinate	Non-orthogonal
Discretization Method	Finite volume
Numerical Scheme	SIMPLE
Turbulent Model	k-ε model

Idealizing and Realizing Approach

In order to apply MASCOT to climate assessment appropriately, it needs to introduce Idealizing and Realizing Approach (IRA). Figure 3 shows the concept of IRA. The mesoscale wind climate was first idealized to the virtual wind climate over virtual flat terrain to exclude the terrain effect using the result of numerical simulation over rough terrain (Figure 3(a)). Then virtual wind climate was realized to the microscale wind climate by including the effect of microscale terrain using the result of numerical simulation over fine terrain (Figure 3(b)). By this approach, correction factor C_t can be estimated.

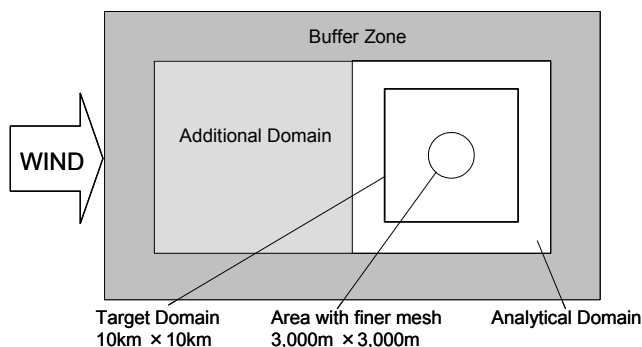


Figure 2. Computational domain

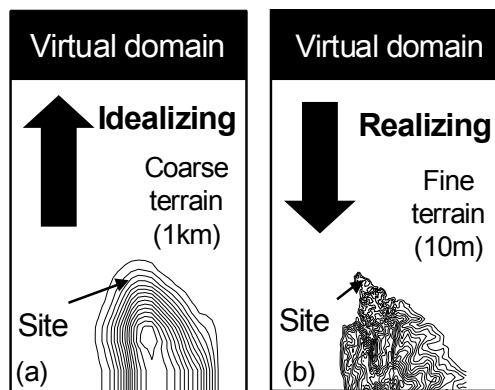


Figure 3. The concept of IRA

Table 6. The details of the computation

Number of wind direction sectors		16
Resolution of Numerical Terrain Map	wide area	50m
	narrow area	10m
Resolution of the Map of Surface Roughness		100m
Analytical domain	Horizontal X × Y	10,000m × 10,000m
	Vertical Z	1,500m
Area of the minimum mesh		3,000m × 3,000m
The minimum interval of mesh	Horizontal	20m
	Perpendicular	5m
The maximum interval of mesh		200m

The Wind Tunnel Test

Since the railway structures such as wind fences, embankments, and bridges cannot be considered in the numerical simulation even with minimum resolution, appropriate consideration of the structures could improve the wind prediction. Thus, the effects of the wind fences, the embankment and the bridge on the wind speed were evaluated by wind tunnel tests, and measured wind speed ratios were considered in addition to the non-linear flow simulations. Figure 4 and Table 7 show the wind tunnel and the conditions of the test. One of the measurement sites, the site 1, is a relatively high embankment with wind fences, and the site 2 is a bridge with fence. Figure 5 and Figure 6 show the cross sections of models of these structures.



Fig. 4. The wind tunnel

Table 7. Wind tunnel test

Wind tunnel	Width	1.5m
	Height	1.8m
Wind tunnel test	Scale	1/40
	Wind Speed Profile	Power law $\alpha=1/7$
	Wind speed	9 m/s
	Measurement sensor	X-wire

Measured wind speed ratio by the wind tunnel test with respect to the site 1 and the site 2 are shown in Figure 7. From Figure 7(a), it can be said that the winds are accelerated by the embankment. In addition, the fence lies on the East South East direction of the railway can work effectively to prevent the wind, although the wind from the West North West direction has few effect of the wind fence because the anemometer was installed just above the fence. It is also found from Figure 7(b) that the effects of the wind fences on the bridge are similar to that on the embankment. By these tests, correction factors C_s and C_b can be estimated.

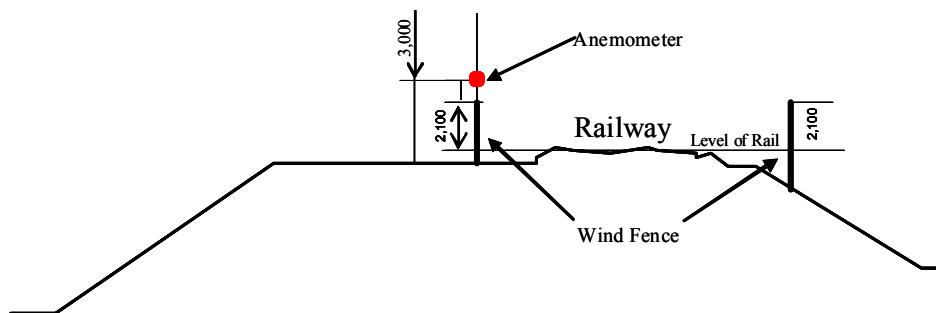


Figure 5. Shape of the cross section of embankment at Site 1

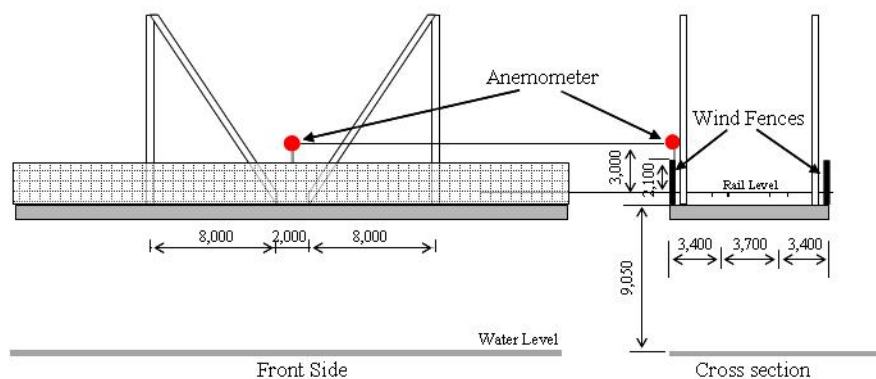


Figure 6. Shape of bridge at Site 2

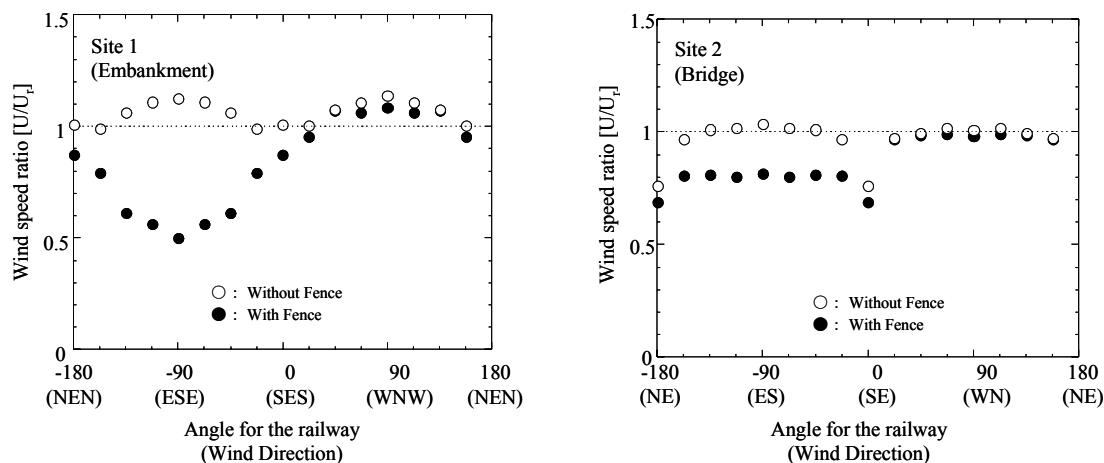


Figure 7. The effect of the structures and the wind fences (site1 and site 2)

Verification of the proposed wind prediction model

In order to verify the wind prediction models, the results of the proposed model were compared with the empirical model and the measured wind speeds at the sites. The estimated frequency distributions of the wind speed and the annual average wind speeds by directions for each site are shown in Figure 8, 9, and 10. The annual mean wind speeds and prediction errors are shown in Table 8.

At the site 3, where there is no remarkable structure, the predicted frequency distributions and annual average wind speeds by the proposed model are in good agreement with the measurement, and the prediction error is 7%. This is because that Dynamical Statistical Downscaling Procedure can consider the small scale terrain around the site.

Because of the existence of the wind fences, the embankment, and bridge, the prediction results by Dynamical Statistical Downscaling Procedure at the site 1 and the site 2 still overestimate the wind speeds. By considering the effects of these obstacles using the results of the wind tunnel test, the estimated wind climate at the site 1 and the site 2 show better agreement with the measurement. The prediction errors of annual mean wind speed at the site 1 and the site 2 are 58% and 46% respectively. One of the reasons of the inconsistencies can be the effects of surrounding buildings and vegetations.

Table 8. Average wind speed of observations and estimation results

	Annual average wind speed					
	Site1		Site 2		Site 3	
	[m/s]	error[%]	[m/s]	error[%]	[m/s]	error[%]
Measurement	1.60	—	2.20	—	2.24	—
Mesoscale database + empirical model	3.96	148%	3.26	49%	3.06	37%
Mesoscale database +DSDP with MASCOT	2.95	84%	3.61	64%	2.39	7%
Mesoscale database + DSDP with MASCOT + Wind tunnel test	2.52	58%	3.21	46%	—	—

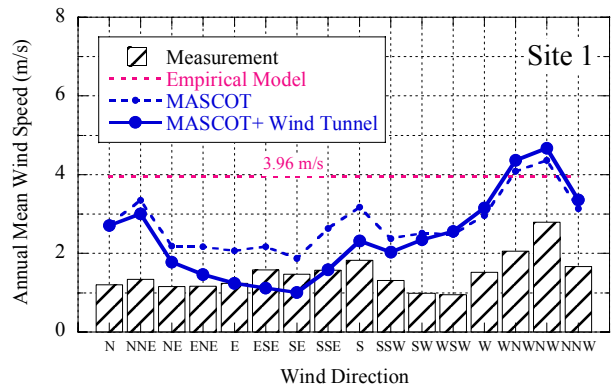
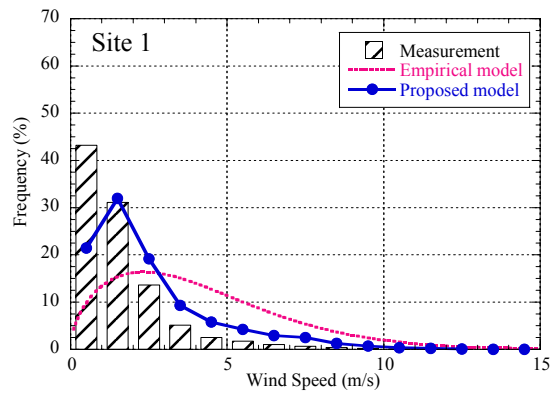


Figure 8. Frequency distributions of wind speed and annual mean wind speed by directions (site 1)

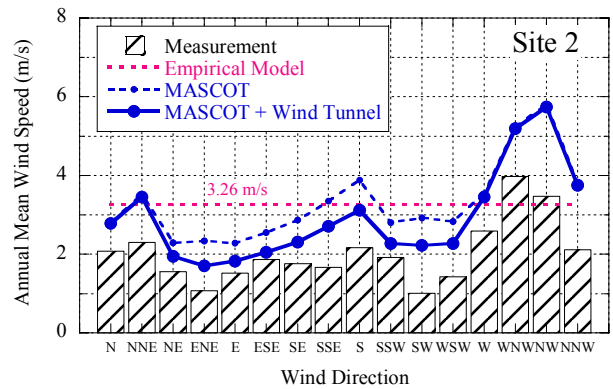
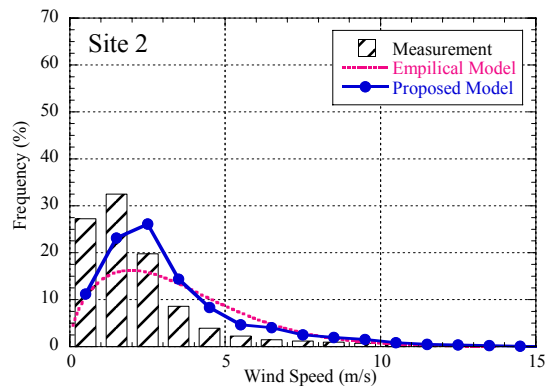


Figure 9. Frequency distributions of wind speed and annual mean wind speed by directions (site 2)

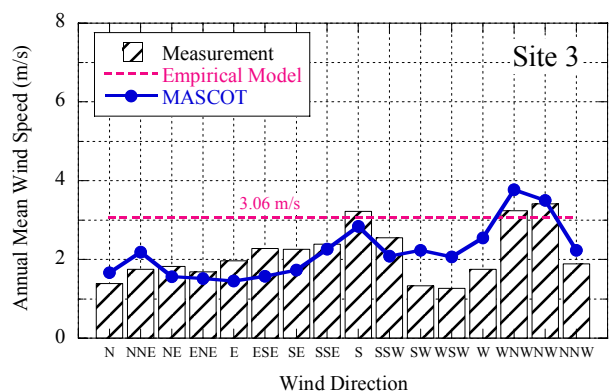
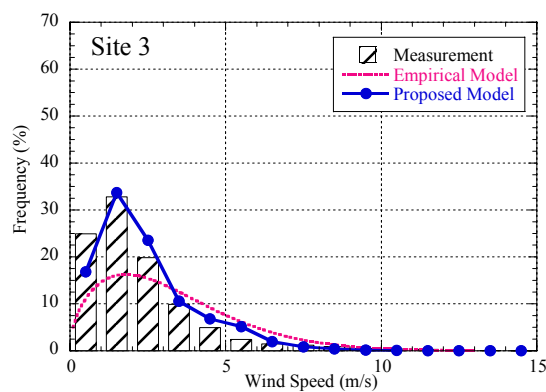


Figure 10. Frequency distributions of wind speed and annual mean wind speed by directions (site 3)

Conclusions

In this study, the applicability of Dynamical Statistical Downscaling Procedure to the wind prediction along railway was investigated. Following results were obtained.

1. By Dynamical Statistical Downscaling Procedure, the prediction of the wind climate at any sites along the railway track in Japan was made possible. The predicted result especially at the site 3, where there is no significant large structure such as embankment, bridge, and wind fences, shows better agreement with the measurement than simply using the mesoscale wind climate database and the empirical formula. Prediction error of annual mean wind speed at the site 3 is 6.7%.
2. By considering the effects of the surrounding obstacles, like embankment, bridge, and fences, by the wind tunnel test, the prediction accuracy was improved. The prediction errors of annual mean wind speed at the site 1 and the site 2 can be reduced to 58% and 46% from 84% and 64% respectively.
3. One of the reasons of the inconsistencies between the measurement and the prediction at the site 1 and site 2 can be the effects of surrounding buildings and vegetations.

References

- Architectural Institute of Japan, (2004), "Recommendation for Loads on Buildings", Japan
- European Convention for Constructional Steelwork, (1978) "Recommendations for the Calculation of Wind Effects on Buildings and Structures", Brussels.
- Ishihara, T., Yamaguchi, A., and Fujino, Y., (2003) "A nonlinear model MASCOT: development and application", Proc. of 2003 European Energy Conference and Exhibition, Madrid.
- Tani, N. (1974), "Handbook of the meteorology for the agriculture, Wind Brakes and Fences", 628-633.
- Yamaguchi, A., and Ishihara, T., (2003), "A Dynamical Statistical Downscaling Procedure for Wind Climate Assessment", 2003 European Wind Energy Conference, Madrid.